Reorientation and Allied Dynamics in Water and Aqueous Solutions

Damien Laage,[1] Guillaume Stirnemann,[1]
Fabio Sterpone,[1] Rossend Rey,[2] and James T. Hynes[1,3]

[1] Department of Chemistry, Ecole Normale Supérieure, UMR ENS-CNRS-UPMC 8640, 75005 Paris, France; email: damien.laage@ens.fr

[2] Departament de Física i Enginyeria Nuclear, Universitat Politècnica de Catalunya, Barcelona 08034, Spain; email: rosendo.rey@upc.edu

[3] Department of Chemistry and Biochemistry, University of Colorado, Boulder, Colorado 80309-0215; email: hynes@spot.colorado.edu

Keywords

hydrogen bonds, angular jumps, hydration dynamics

Abstract

The reorientation of a water molecule is important for a host of phenomena, ranging over—in an only partial listing—the key dynamic hydrogen-bond network restructuring of water itself, aqueous solution chemical reaction mechanisms and rates, ion transport in aqueous solution and membranes, protein folding, and enzymatic activity. This review focuses on water reorientation and related dynamics in pure water, and for aqueous solutes with hydrophobic, hydrophilic, and amphiphilic character, ranging from tetramethylurea to halide ions and amino acids. Attention is given to the application of theory, simulation, and experiment in the probing of these dynamics, in usefully describing them, and in assessing the description. Special emphasis is placed on a novel sudden, large-amplitude jump mechanism for water reorientation, which contrasts with the commonly assumed Debye rotational diffusion mechanism, characterized by small-amplitude angular motion. Some open questions and directions for further research are also discussed.

1. INTRODUCTION

This review focuses on the question, how does a water molecule reorient in water and around solutes in aqueous solution? It seems fair to say that the majority view of the mechanism of water reorientation has been that of rotational diffusion, introduced long ago by Debye (1). Here the water molecule changes its orientation in very small angular steps, in a diffusive fashion. As we discuss below, recent theoretical and experimental work argue for a quite different picture in which the water molecule reorients predominantly via a mechanism involving sudden, large-amplitude jumps. This picture is discussed below for pure water and aqueous solutions involving ions, hydrophobic molecules, and amino acids, with attention given to theory, simulation, and assorted experimental probes, as well as to reorientation-related phenomena including, e.g., hydrogen-bond (HB) breaking and making, HB exchange, and vibrational dephasing.

Why is the question important? For pure water, reorientation is intimately connected with the dynamic rearrangement and restructuring of the HB network, a key aspect for water's unique properties. The significance of water reorientation in the hydration shells of various solutes, more fully detailed below, ranges from its importance for, e.g., ion transport to protein folding. Perhaps less familiar for water reorientation is its importance for assorted chemical reaction classes in aqueous solution. One example is S_N2 reactions, e.g., $X^- + RY \rightarrow XR + Y^-$, in which water reorientation is an important part of the prior solvent rearrangement necessary to reach the reaction transition state (TS) (2). Other examples are provided by acid dissociation proton transfer reactions (3, 4) and proton transport (5–7). For the former, illustrated schematically by the proton transfer $AH \cdots H_2O \rightarrow A^- \cdots H_3O^+$ within an HB pair, the reaction coordinate involves a change in the coordination number of the proton-accepting water from 4 to 3, involving water reorientation to break a donor HB to the water (3, 4). For the latter, schematically $H_3O^+ \cdots H_2O \rightarrow H_2O \cdots H_3O^+$, there is an additional and analogous 3 to 4 number change for the proton donor site (3–7).

Our detailed review begins in Section 2, devoted to pure water, and continues in Section 3, addressed to water reorientation in the hydration layer of various solutes. Concluding remarks are offered in Section 4.

2. REORIENTATION IN PURE WATER

2.1. Orientation Time-Correlation Function

The simplest description of a water molecule's reorientation kinetics relies on the time-correlation function (TCF) of the molecular orientation. For a given body-fixed vector such as the water OH bond or dipole moment, this function tracks how fast memory of the initial orientation is lost. Its definition is

$$C_n(t) = \langle P_n[\mathbf{u}(0) \cdot \mathbf{u}(t)] \rangle, \tag{1}$$

where P_n is the Legendre polynomial of rank n, and $\mathbf{u}(t)$ is the molecular orientation at time t. A typical example of such an orientation TCF for bulk water at room temperature is shown in **Figure 1**. On a logarithmic scale, this function shows that water reorientation proceeds successively at different rates, and thus with different mechanisms: It exhibits a fast (subpicosecond) partial reorientation, followed by a slower (picosecond) full reorientation. Before discussing these mechanisms, we pause to survey the main techniques available to probe water reorientation dynamics.
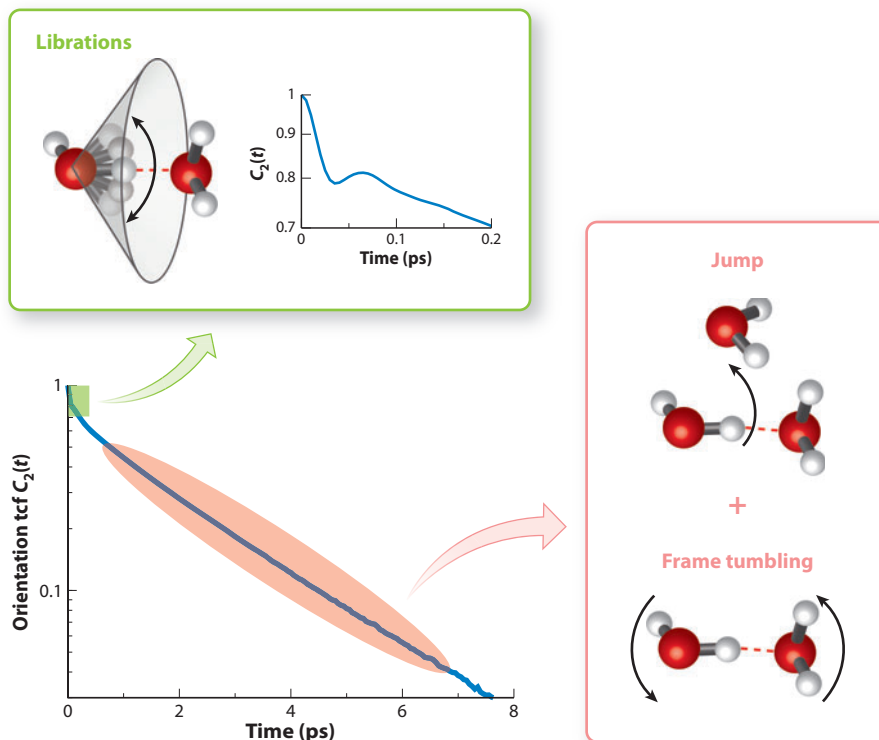
Figure 1

Second-rank orientation time-correlation function $C_2(t)$ (Equation 1) for a water OH bond at room temperature determined through molecular dynamics simulations (35). For each time regime, the key reorientation mechanisms are indicated.

2.2. How to Measure the Reorientation

Currently, the most information-rich technique to probe water reorientation dynamics is infrared (IR) pump-probe spectroscopy (8–15), which possesses the necessary femtosecond time resolution to follow the very fast water reorientation motions. By combining the signals collected with parallel and perpendicular polarizations of the pump and probe pulses, one recovers the anisotropy decay of this population, usually approximated as $2/5 \times C_2(t)$ (15, 16) (see Equation 1). Despite this technique's great value, several limitations exist. First, the anisotropy cannot be reliably measured for delays much longer than the vibrational lifetime (<10 ps). Second, the anisotropy-orientation TCF connection is not as straightforward as usually assumed; additional effects [e.g., non-Condon effects (17) and distributions of vibrational lifetimes (17, 18)] must be included for a quantitative comparison.

Nuclear magnetic resonance (NMR) spectroscopy can also provide information on the re-orientation dynamics through measurement of the spin-lattice relaxation time, which is partly determined by rotational relaxation (19–23). However, NMR is not sufficiently time resolved to follow the water dynamics in the time domain; the measured relaxation time is the orientational TCF time integral $\langle \tau_2 \rangle = \int_0^\infty C_2(t)dt$, which corresponds to a weighted average of the reorientation times of the different mechanisms (19). Deuterium NMR in D_2O probes the OD bond

Vibrational lifetime: population relaxation time constant of an excited vibration, e.g., here the water OH stretch

Non-Condon effect: dependency of the vibrational transition dipole moment of a given molecule on the arrangement of the surrounding molecules

reorientation, proton NMR in H_2O probes the HH intramolecular vector reorientation, and ^{17}O NMR probes the reorientation of the vector orthogonal to the molecular plane (23–25).

Quasi-elastic neutron scattering (QENS) follows the motions of individual hydrogens and has been used to investigate water rotational dynamics (26–28). However, it assumes decoupled water translational and rotational motions [not rigorously exact (29)] and postulates a model for the small-amplitude translational displacements. The resulting rotational component of QENS spectra is sensitive to the reorientation times associated with Legendre polynomials of increasing order ($\tau_1, \tau_2, \ldots$). The interpretation of these spectra was recently shown to be extremely dependent on the chosen reorientation model (30).

Several other experimental techniques probe water's collective reorientation dynamics, including terahertz spectroscopy, dielectric relaxation (31, 32), and optical Kerr-effect spectroscopy (33). However, because reorientations of individual molecules are coupled and more than one mechanism contributes to the reorientation, there is no simple relationship between the collective and single-molecule reorientation times. The Debye relaxation time is, for example, almost twice as long as the first-order molecular reorientation time τ_1 at room temperature (31, 34, 35).

Many other powerful techniques have been used to investigate water dynamics without specifically probing reorientation, including, e.g., time-dependent Stokes-shift (36), two-dimensional (2D) IR (37, 38), and terahertz (39) spectroscopies. Molecular dynamics (MD) simulations are also a valuable tool to investigate water reorientation dynamics, as they both provide a molecular-scale description of the water motions and can be used to calculate the experimental observables detailed above. Several descriptions have been employed, including, e.g., classical MD with water geometries that are rigid (35, 40, 41) or not (18), in which polarizability is included (18) or not (35, 40, 41); centroid MD, which describes explicitly the quantum nature of the hydrogen motion (42); and first-principles MD (43, 44) in which the electronic structure is calculated by density functional theory.

All calculated orientational TCFs exhibit the same general behavior as in **Figure 1**, although the relaxation times are slightly model dependent. The great (potential) advantage of simulations is the provision of a molecular picture explaining the experimental measurements.

2.3. Subpicosecond Reorientation: Librations

We now return to the discussion of the TCF decay displayed in **Figure 1**. The initial decay results from the water molecule's inertial rotational motion, rapidly hindered by the HBs with the nearest neighbors, which exert restoring torques around an average orientation: This is illustrated by the initially underdamped decay (see the inset in **Figure 1**). These librational motions therefore cause a fast (<200 fs) but limited reorientation, as each water OH bond executes a wobbling motion in a cone whose axis is the HB donor-acceptor direction (16, 45–47). The semiangle of the cone is inversely proportional to the HB strength, with a stronger HB leading to a tighter cone (13, 47).

This librational decay can be measured by pump-probe spectroscopy. By varying the pump and probe frequencies (8, 10, 14), systems with different HB strengths are selected. This explains why blue-shifted frequencies, which excite OH bonds engaged in weaker HBs that librate in a wider cone, lead to a larger amplitude of the librational anisotropy decay (40, 47).

Several aspects of this librational decay remain unclear and continue to be investigated. These include, for example, the discrepancy between librational decay amplitudes measured via polarization-resolved pump-probe spectroscopy and simulated orientational TCFs (13). Possible explanations include the role of resonant vibrational energy transfer between excited OH vibrations (48, 49), non-Condon effects causing the orientational TCF to not rigorously equal the anisotropy (17), and nuclear quantum effects (42). The role of temperature is also under investigation,

QENS: quasi-elastic neutron scattering

Two-dimensional infrared (2D-IR) spectrum: infrared spectrum representing the correlation between excitation and detection frequencies separated by a given delay

MD: molecular dynamics

**Libration:** hindered OH rotation around its hydrogen-bond axis

stimulated by the first experiments indicating a transition from an OH excitation frequency-dependent initial rapid anisotropy drop at room temperature to a frequency-independent drop around the freezing point (13).

2.4. Picosecond Reorientation: Angular Jumps and Frame Tumbling

We now turn to the longer-time (greater than picosecond) decay of the orientation TCF. As mentioned in Section 1, this orientational relaxation has been commonly described by the Debye rotational diffusion picture (1), an angular Brownian motion of the water molecules through very small angular steps. Although this description had been sporadically questioned (33, 50–54), it is only recently that a combination of theoretical and experimental breakthroughs has provided consistent evidence suggesting a dominant reorientation via a quite different mechanism involving large-amplitude sudden angular jumps.

2.4.1. Jumps. An MD study provided the first detailed, quantitative, molecular description of water reorientation, providing evidence that the picosecond reorientation of water results from large-amplitude angular jumps when a water OH trades HB acceptors (35, 41). This exchange process, which can be viewed fruitfully as a chemical reaction, is depicted in **Figure 2**. The first step is the initial HB's elongation while a new water oxygen acceptor approaches, in most cases from
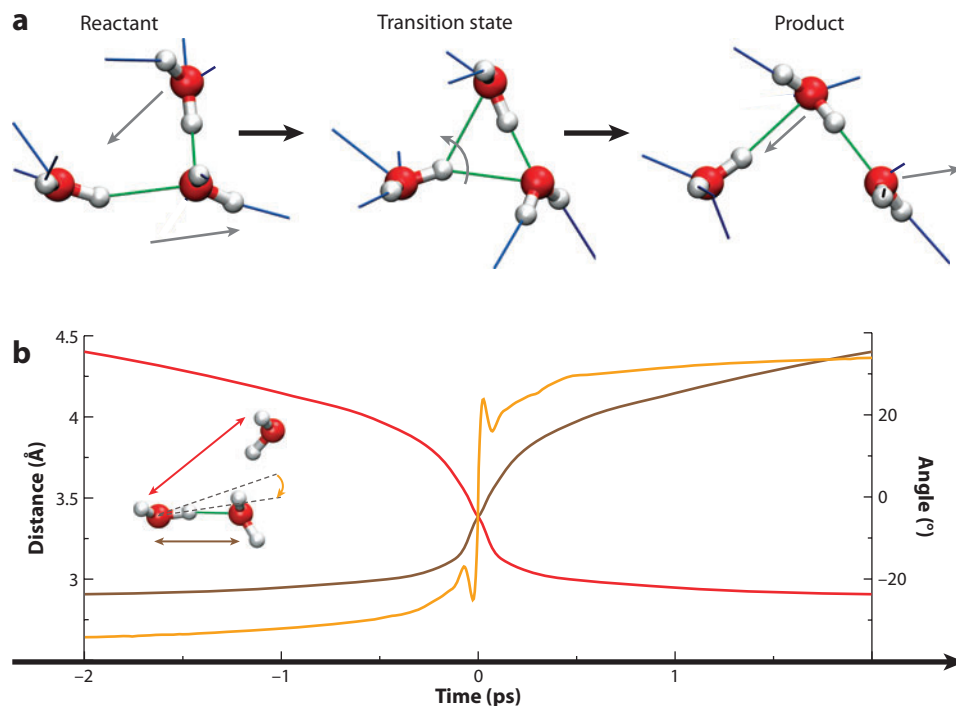
Figure 2

(*a*) Schematic jump reorientation mechanism (for a detailed description, see 35). (*b*) Time dependency of three geometrical parameters—distance to the initial acceptor (*brown line*) and to the final acceptor (*red line*), and angle with respect to the bisector plane (*yellow line*)—along the average jump path (35), where the system crosses the transition state at time 0.

the second shell. Once the initial and final oxygen acceptors are equidistant from the rotating water oxygen, the water OH can suddenly execute a large-amplitude angular jump from one acceptor to another, and at the TS for this HB exchange, the rotating water forms a symmetric bifurcated HB with its initial and final water acceptors. The HB with the new partner eventually stabilizes, while the initial partner leaves. This jump mechanism's free energy barrier was shown from simulations to originate not only from the initial HB's elongation, but also from the new partner's penetration into the first shell (35); this jump barrier is smaller than the free energy cost to fully break the initial HB because of the mechanism's concerted nature. Explicitly treating the hydrogen motion's quantum character is not expected to produce a qualitative mechanistic change (35) but deserves attention.

Obviously, the mechanism shown in **Figure 2** is to be understood as an average, simplified, but representative mechanism. Actual paths are distributed around this typical mechanism, as illustrated by the wide jump angle distribution found (35) around the average amplitude of 68°. Such a jump mechanism is consistent with, but distinct from, prior studies on related aspects of water dynamics, both experimental and theoretical, including, e.g., those on the HB lifetime (55, 56), the importance of five-coordinated structural defects in enhancing the translational mobility (57), and the unstable and transient character of dangling OHs (38). A detailed discussion of the relation and differences between the jump mechanism and a number of these studies may be found in Reference 35.

The consequence of these angular jumps in the orientation TCF can be determined through the jump model developed by Ivanov (58), which generalizes the diffusive angular Brownian motion picture to finite-amplitude jumps. It assumes that the jumps have a constant amplitude, are uncorrelated, and occur with a frequency of $1/\tau_{\text{jump}}$ around axes distributed isotropically. This model and its specificities with respect to other reorientation models are discussed, for example, in Reference 59.

Within the Ivanov model, the n-th order reorientation time of the orientation TCF given in Equation 1 is

$$\tau_n^{\text{jump}} = \tau_{\text{jump}} \left\{ 1 - \frac{1}{2n+1} \frac{\sin[(n+1/2)\Delta\theta]}{\sin(\Delta\theta/2)} \right\}^{-1}, \qquad (2)$$

where $\Delta\theta$ is the jump amplitude, which can be determined from simulations, together with the now microscopically identified jump time τ_{jump} (58) [at 300 K, $\tau_{\text{jump}} = 3.3$ ps and $\Delta\theta \simeq 68°$ (35)].

2.4.2. Extended jump model. This simple jump model, however, is incomplete because it assumes that the molecular orientation remains fixed between jumps. For water, this would imply that, while a water OH bond retains the same HB acceptor, the OH direction remains frozen. On subpicosecond timescales, this is not the case because of the librational motions described above, nor is it the case on the slower picosecond timescale because of the reorientation of the intact HB axis through a tumbling motion of the local molecular frame.

The jump and frame contributions are combined within an extended jump model (EJM) (35, 41). Because the jump and frame motions are independent, the resulting TCF is the product of the two TCFs, and the overall EJM reorientation time is (35, 41)

$$\frac{1}{\tau_n^{\text{EJM}}} = \frac{1}{\tau_n^{\text{jump}}} + \frac{1}{\tau_n^{\text{frame}}}. \qquad (3)$$

The reorientation time is dominated by the faster jump contribution [from simulations with the SPC/E water force field at 300 K, $\tau_2^{\text{EJM}} = 2.2$ ps, $\tau_2^{\text{jump}} = 3.6$ ps, and $\tau_2^{\text{frame}} = 5.6$ ps (35)]. The resulting EJM provides an excellent description of the timescales measured, e.g., by ultrafast IR and NMR spectroscopies, and by simulations.

2.4.3. Hydrogen-bond network dynamics. The jump mechanism focuses on the replacement of one HB acceptor by another and thus offers a local perspective on the way the water HB network reorganizes and changes its connectivity. However, such a local jump requires the approach of the new partner and the departure of the former partner, both necessitating second shell rearrangements (35, 41). This therefore implies collective motions involving molecules beyond the three water molecules depicted in the mechanism given in **Figure 2**. The jump mechanism thus provides a local mechanistic view of water's collective HB network rearrangements (60).

Several timescales have been suggested to characterize water's HB network dynamics, each focusing on one aspect of the dynamics. The continuous HB lifetime (55, 56, 61), i.e., the time until an HB first breaks, usually through a large-amplitude libration, provides an HB strength measure. Most of these breakings are transient, and the original HB is quickly reformed. The HB acceptor exchange time (i.e., the jump time discussed above) measures the time to go from an initial stable HB to another stable HB with a different acceptor and thus measures the timescale of stable rearrangements of the HB network. It is the inverse of the forward HB exchange rate constant and depends both on the initial HB strength and the availability of a new partner. A third timescale is the intermittent HB lifetime (55, 56, 61, 62), which measures the survival probability of an initially hydrogen-bonded pair. This time reflects the diffusion of the initially hydrogen-bonded pair (56). It includes a contribution from the backreaction reforming the original bond, even when a new stable HB was formed in between. The values for these timescales determined from SPC/E water simulations at 298 K differ markedly: $\tau_{cont} = 0.5$ ps (63), $\tau_{jump} = 3.3$ ps (35), and $\tau_{int} = 6.5$ ps (63).

2.4.4. Experimental support. Direct experimental evidence showing the existence of the angular jumps in neat water has so far remained elusive. The second-order reorientation time (i.e. corresponding to the second-order Legendre polynomial in Equation 1) measured by NMR and ultrafast IR spectroscopies cannot readily discriminate between diffusive and jump models, and its ratio with the first- or third-order times is needed (see Equation 1). Unfortunately, these times are presently not directly accessible experimentally. However, several less direct results support the jump picture. First, 2D-IR spectroscopy revealed the transient character of non-HB states (38), which is fully consistent with the jump mechanism in which HB acceptor exchange occurs through the concerted breaking and forming of HBs. Additional evidence comes from QENS, which is sensitive to both the first- and second-order reorientation times (26). The surprising twofold difference between the second-order reorientation times obtained from QENS and from NMR and ultrafast IR spectroscopies disappears when the angular jump model replaces the rotational diffusion assumption to interpret the spectra (30). The bifurcated HB configuration of the jump TS (**Figure 2**) also explains why five-coordinated water molecules exhibit an increased mobility (57) and why the water translational diffusion constant first increases with increasing pressure (20). A higher pressure facilitates the formation of the bifurcated HB configurations and thus the HB exchanges necessary for a translational displacement. Furthermore, a recent frequency-dependent extension of the EJM (64) predicted that the anisotropy decay of water OHs, which are initially weakly hydrogen bonded, exhibits a moderately faster decay in the 0.5–3-ps range due to the increased probability to undergo a jump for these systems. This behavior has been observed both in simulations (40, 42, 47, 64) and polarization-resolved pump-probe experiments (8, 14).

To date, the clearest indications of the presence of angular jumps have been obtained in ionic aqueous solutions. 2D-IR spectroscopy experiments have recently measured the exchange time from an anion acceptor to a water acceptor (65, 66), and the angular amplitude of such exchange (67), leading to values in excellent agreement with the EJM predictions (18).

2.4.5. Frequency dephasing. The dephasing or memory loss of the OH frequency, as characterized by the fluctuating OH frequency TCF or otherwise (40, 68, 69), is related to water's angular motion because the frequency is sensitive to the OH orientation in an HB (40, 68, 69). As extensive recent reviews exist (15, 70, 71), we make only limited comments here for water, with additional remarks allocated to subsequent sections.

The longer-time $\sim$1–2-ps decay of, e.g., the TCF has been interpreted as resulting from transient HB breaking and making (15, 40, 68, 69), which would involve large-amplitude librations rather than full water molecule reorientation. The great similarity (72) of calculated water 2D-IR spectra when jumps are excluded or not provides further evidence that water spectral dynamics is mostly determined by transient HB breakings, corresponding to unsuccessful jump attempts in which the OH returns to its initial acceptor. An alternate suggestion (73) is that dephasing results from collective motions. These two current views are not necessarily incompatible (73), and further elucidation would be valuable.

3. REORIENTATION AROUND SOLUTES

3.1. How to Measure the Influence of a Solute?

Understanding the water reorientation mechanism in neat water, although interesting per se, also provides a reference to assess how a solute influences the dynamics of the surrounding water molecules. Measuring a solute's influence on the hydration shell dynamics is a long-standing issue in experiments, theory, and simulations, and different strategies have been developed.

Most experiments, including, e.g., NMR, QENS, and ultrafast IR spectroscopy, collect a signal resulting from water molecules both within the hydration layer and in the bulk, and separating the two contributions is challenging. Some NMR experiments (22, 74, 75) employ dilute solutions (e.g., below 1 M) in which a two-state picture (hydration shell and bulk) is probably valid, and the hydration-layer contribution is inferred from a concentration-dependency study. Such results, however, are intrinsically averaged over the entire hydration layer and require the knowledge of the number of water molecules within this layer. Other NMR techniques have also been used more specifically for biomolecule hydration (76, 77). QENS studies have estimated the dynamics within the solute hydration layer by comparing spectra recorded at high (2 M) and low (0.5 M) concentrations (27). A significant limitation here is the assumption that the hydration-layer dynamics is independent of concentration even at high concentrations. Some ultrafast IR spectroscopy experiments exploited the longer water OH stretch vibrational lifetime within some solute hydration shells (e.g., anions) compared to the bulk situation (78). This ensured that past a certain delay the signal would mostly originate from hydration-layer molecules; however, subsequently this was shown to lead to artifacts in the reorientation time determination (18). An alternate procedure relies on concentration-dependent studies (79), but because of sensitivity issues, these studies require concentrated solutions (>1 M) in which the simple two-state hydration shell-bulk picture is invalid (80).

MD simulations also face difficulties in identifying the specific dynamics of water molecules within a solute hydration layer. First, the hydration-layer definition may be ambiguous, and different procedures have been suggested (81). Second, when the shell is labile, reorientation and departure from the shell occur on similar timescales (82). The interpretation of an orientational TCF for a water molecule initially in the first shell is therefore not unambiguous because this molecule may leave the shell. Because, as detailed below, for several solutes water reorientation proceeds through HB exchange and departure from the first to the second shell (18, 80), focusing on molecules continuously residing in the shell could then yield an artificially slow reorientation time as this would exclude the jump reorientation out of the shell.

As discussed below, all these considerations are relevant to understand and rationalize the sometimes disparate results obtained with different techniques.

3.2. Hydrophobic Solutes

Water's peculiar behavior around hydrophobic solutes is among its most unusual properties (50, 83–87). One of its spectacular and most important manifestations is the water-mediated hydrophobic interaction between apolar solutes in aqueous solution (84, 87), which plays a key role in a wide range of chemical and biochemical processes, furnishing, for example, the driving force for protein folding and for the self-assembly of lipids into membranes (83, 88). Hydrophobic interaction and hydration have been extensively studied, and their structural and thermodynamic aspects are now much better understood (84–87, 89, 90). However, a comparable comprehension of water dynamics next to hydrophobic solutes, which can play a decisive role, e.g., in protein folding and (bio)molecular recognition (36, 88), remains elusive and controversial. We review below some recent aspects of this issue, focusing on the immobilized versus moderately retarded character of water dynamics around hydrophobic groups, and discuss how a simple model (80) can rationalize the contradictory conclusions reached by time-resolved measurements (79), NMR (22, 75, 91–94), and simulations (44, 51, 72, 80).

3.2.1. Iceberg versus moderate slowdown.
Hydrophobic compounds are weakly soluble in water because of a surprisingly large loss of entropy compared with other solvents (84). These thermodynamic observations were interpreted in 1945 by Frank & Evans (95) as arising from the formation of crystalline structures around apolar groups, introducing the picturesque iceberg term to refer to such frozen water molecules (95). Although appealing, this model has been seriously challenged (83, 84), mostly because there has never been evidence of enhanced ice-like structures in either neutron scattering experiments (96) or simulations (84) under ambient conditions, and because the entropy loss can be explained without invoking such icebergs (97).

However, the recent first time-resolved measurements of water reorientation in the hydration shell of amphiphilic molecules (79) were interpreted as supporting the iceberg concept from a dynamical, as opposed to structural, point of view. The observation of a large residual anisotropy after a delay (well beyond the 2.5-ps bulk water reorientation time) was assigned to the immobilization of four water OHs per methyl group, independent of the solute concentration (79). Subsequent 2D-IR experiments (98) and proton mobility measurements (99) on the same solutions were interpreted via the same picture. According to these studies, the jump exchange of HB acceptors is suppressed for some hydration shell water molecules, preventing their reorientation and strongly slowing down related phenomena, including proton mobility and OH vibrational dephasing. As discussed below, an alternate interpretation of these experiments without invoking any immobilization has been advocated (72, 80), but the aforementioned studies already raise several questions. For example, only a fraction of the first shell water OHs are immobilized, whereas the others would exhibit bulk-like dynamics; this stark contrast is intriguing. In addition, the interpretation of these experiments assumed the presence of a bulk water population even at concentrations close to the solute saturation, which does not seem realistic.

This dynamic iceberg picture contrasts strongly with the conclusions of earlier NMR (22, 91–94) and dielectric relaxation experiments (100) on a wide span of solutes, ranging from pure hydrophobes [e.g., xenon (91)] to amphiphiles [alcohols (75, 92, 94), methylated urea (22, 93), and small peptides (22)]. In all these experimental studies, together with all MD simulations performed with a large variety of force fields (44, 51, 72, 80), it was concluded that water reorientation is only

moderately slowed in the hydration shell for dilute solutions: The retardation referenced to bulk water rarely exceeds a factor of 2.

Although experiments only measure a reorientation time averaged over all the water OHs lying in the hydration layer, simulations have the ability to spatially resolve the dynamics according to the different orientations of the water OHs, distinguishing in the clathrate hydration structure (85) between those tangent to the hydrophobic group and those pointing toward the bulk. A systematic classical MD study showed that outward pointing OHs exhibit bulk-like dynamics, whereas initially tangent OHs are retarded by a factor close to 1.5 that seems little sensitive to the nature of the hydrophobe (80); no water immobilization was found. Similar conclusions have been reached by ab initio MD simulations (44).

3.2.2. Transition-state excluded-volume effect.
The seemingly contradictory observations between ultrafast IR spectroscopy and other techniques can be reconciled and rationalized within the EJM framework in terms of a transition-state excluded-volume (TSEV) effect for HB exchange, without invoking any water immobilization (80). The EJM framework provides a quantification of the steric effect induced by small hydrophobes, some aspects of which had been qualitatively recognized earlier (57, 101).

The slower reorientation dynamics around hydrophobes is found to essentially result from a 1.5-fold slowdown of the HB exchanges (72, 80). Despite this moderate retardation, the average jump mechanism is identical to that in the bulk, and the system thus does not pass through a higher-energy TS. However, the approach of a new HB acceptor, which is an important contributor to the reaction rate-limiting step, is hindered by the presence of the hydrophobic solute, inducing an excluded volume. Consequently, the number of accessible TS configurations is reduced. This effect can be quantified by considering that a fraction f of the ring representing the TS location (defined in the bulk by a distance $R^{\ddagger}$ to the reorienting water and a $\Delta\theta$ jump angle) overlaps with the hydrophobic solute excluded volume (see **Figure 3**). Simple TS theory considerations then lead to the TSEV slowdown factor ρ_V, the ratio between the jump time $\tau_{jump}^{hydrophobe}$ for an OH in the hydrophobe hydration shell and the jump time in bulk τ_{jump}^{bulk} (80),
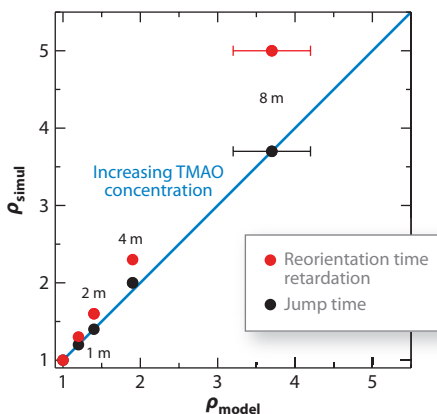
$$\rho_V = \frac{\tau_{jump}^{hydrophobe}}{\tau_{jump}^{bulk}} = \frac{1}{1-f}. \qquad (4)$$

Next to convex interfaces, as for tangent water OHs around hydrophobes, f does not exceed 1/2 (**Figure 3a**), and $\rho_V < 2$. For usual hydrophobic groups (radius 3–5 Å), ρ_V varies little, remaining close to 1.4, in excellent agreement with the simulated retardation factor for a wide range of hydrophobic solutes (80). This TSEV model thus rationalizes a hydrophobic solute's limited effect on water reorientation dynamics observed in NMR and simulations. It has also been successfully applied to an extended hydrophobic surface, for which f is close to 1/2 and thus ρ_V is approximately 1.8 (102).

The TSEV model can also rationalize the seemingly contradictory results between those obtained from NMR (22, 91–94) and simulations (44, 51, 72, 80) and those obtained from ultrafast IR spectroscopy (79). These latter experiments employ high concentrations of amphiphilic molecules (up to 8 mol kg^{-1}). At such concentrations, water OHs in the solute's hydration shell are surrounded by several solutes. The resulting TSEV fraction can now exceed 1/2 (**Figure 3c**); TSEV considerations were shown to quantitatively explain the overall slowdown of water reorientation with increasing concentration, without invoking any immobilization (80). Such concentration-related effects, together with aggregation phenomena (103, 104), can also explain the observed suppressed proton mobility in these solutions (99). At high concentration, the simple two-state

Clathrate: hydration structure in which one of the water tetrahedron faces lies tangent to the solute molecule

TSEV: transition-state excluded volume

a Single solute ($\rho < 2$)

b
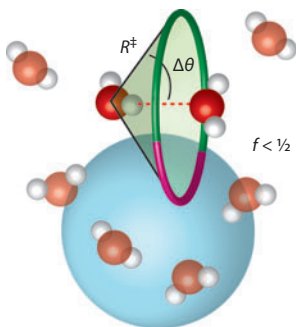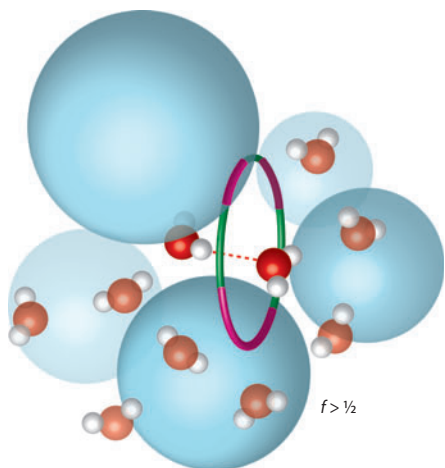
Solute	ρ_{model}	ρ_{simul}
CH_4	1.4	1.2
Xe	1.4	1.2
TMU	1.4	1.3
TMAO	1.5	1.4

c Concentrated solution ($\rho > 2$)

d

Figure 3

Transition-state excluded-volume (TSEV) model: definition of the excluded-volume fraction, model predictions, and simulated jump time retardation for different solutes and concentrations. (*Left panels*) Schematic 3D representation of the excluded-volume fraction for a single solute (*a*) and a concentrated solution (*c*). Considering a stable HB within the hydration shell (*red dashed line*), possible TS locations for the new HB acceptor lie on a ring defined by the distance $R^{\ddagger}$ to the reorienting water and the jump angle $\Delta\theta$. The fraction *f* of this ring overlapping with the solutes is represented in pink, and the complementary accessible fraction is shown in green. (*Right panels*) Comparison between the TSEV model ρ_{model} and the simulation results ρ_{simul} (80); (*b*) for a single solute molecule of methane (CH_4), xenon (Xe), tetramethylurea (TMU), and trimethylamine-N-oxide (TMAO); and (*d*) as a function of concentration for aqueous solutions of TMAO at 1 m, 2 m, 4 m, and 8 m (mol kg^{-1}). At any concentration, the reorientation time retardation (*red dots*) exceeds that of the jump time (*black dots*) because of the frame contribution (Equation 3).

model (bulk/immobilized) used to interpret anisotropy measurements (79) cannot be valid, and one instead finds a broad distribution of dynamical behaviors, depending on the local environment (80).

Finally, the amphiphile's hydrophilic head, which has been ignored in the interpretations of these experimental studies, can in fact play a major role. For increasing solute concentrations, the fraction of water molecules around hydrophilic sites increases. The dramatic slowdown of

vibrational dephasing measured in 2D-IR spectra (98) was argued to originate from the slow chemical exchange between water molecules hydrogen bonded to hydrophilic heads and those hydrogen bonded to other water molecules (72). This slowdown thus results from the hydrophilic head, and not from the hydrophobic moiety as initially suggested (98). As discussed in detail below, the effect of hydrophilic sites or solutes forming an HB with water molecules can be much greater than the rather limited slowdown induced by hydrophobes.

3.2.3. Open questions. Some questions are still debated and deserve future investigation. These include, e.g., the hydrophobic retardation factor's temperature dependency. Ultrafast spectroscopy experiments concluded that the activation energy for water reorientation next to a hydrophobic group at 300 K is double that in bulk (105). This strongly contrasts with NMR results in which, for most hydrophobic solutes, the 300 K activation energy only slightly exceeds the bulk value (22). The activation energy is significantly higher only for hydrophobic ammonium cations (106) and benzene (107), which certainly cannot be regarded as paradigm hydrophobic solutes (108). The TSEV model, which addresses a purely entropic effect, predicts identical activation energies for bulk and hydration shell water reorientation (80): A model refinement accounting for the different water free energies in these locations (89) may lead to the small experimental temperature dependency (22).

3.3. Hydrophilic Solutes

Hydrophobic groups influence water dynamics nearly exclusively through an excluded-volume effect. We now turn our attention to hydrophilic solutes, which interact more strongly with water through HBs and Coulombic interactions.

3.3.1. Anions. Water dynamics around ions is essential for a molecular understanding of, e.g., ion mobility in aqueous solution (109) and ion transport through membranes (110). We focus on anions, especially the halides, which are comparatively simple and experimentally much studied hydrophilic solutes, to investigate how the bulk mechanism of water reorientation through jumps is affected by a solute.

MD simulations of chloride in aqueous solution have provided evidence of large-amplitude angular jumps when a water OH replaces its anion HB acceptor by a water acceptor (18). This HB acceptor exchange leads to the reorienting water's departure out of the anion hydration shell (18). The frame contribution due to the HB axis tumbling between successive jumps adds a slower component to the reorientation (18).

The EJM explains the discrepancy between NMR studies (74), which observe a labile hydration layer around Cl$^-$, and the conclusions of ultrafast IR spectroscopy experiments, which measure a rigid hydration shell (78, 111). In the measured pump-probe anisotropy, the contribution from water molecules, which remain hydrogen bonded to Cl$^-$ (i.e., which only reorient through frame tumbling and do not jump), is overemphasized by their longer water OH vibrational lifetime. Simulations (18) showed that ultrafast IR spectroscopy measures a reorientation time similar to the frame reorientation time, whereas NMR includes the faster jump contribution, which is the main reorientation pathway. [The frame reorientation component, however, will become quite important for small ions such as fluoride (112) or multiply charged ions such as Mg^{2+} (113).] Although it has been suggested (114) that this explanation was inconsistent with the long residence time of chloride's hydration-layer water calculated by ab initio MD simulations, this apparent inconsistency originated from an inadequate calculational procedure for water's residence time

next to labile ions (82). The use of concentrated ionic solutions in pump-probe experiments also renders a comparison with the dilute case more difficult (115).

The longer-time OH frequency dephasing dynamics for water, e.g., weakly hydrogen bonded to an anion such as I^-, can differ from the pure water case (see Section 2.4.5). Due to the frequency blue shift compared to bulk water, a new, longer timescale HB exchange contribution appears (116). Several 2D vibrational photon echo experiments have been performed on aqueous solutions containing anions, including, e.g., BF_4^- and ClO_4^-, which accept very weak HBs from water, leading to a very blue-shifted OH stretch vibrational peak, distinct from the bulk water band, as for I^-. The great advantage is that the anion hydration shell water molecules can be probed specifically; anion shell-bulk exchange can be observed through 2D-IR spectroscopy. Experiments measuring the exchange dynamics (65, 66) on concentrated aqueous solutions yield an exchange timescale totally consistent with the EJM predictions, taking into account the slowdown due to the employed high concentration (18). Recently, the anisotropy decay due to the anion shell-bulk exchange has been measured by 2D-IR spectroscopy (67); the associated angular jump amplitude was determined to be approximately 50°, qualitatively consistent with the 60°–70° amplitude found in simulations (18, 67).

3.3.2. Amino acids. Amino acids are appealing elementary molecules to investigate the influence of small solutes on water reorientation dynamics. Their side chains possess all the minimal components to understand the span of various effects: Some are hydrophobic, whereas others are hydrophilic, and among hydrophilic groups, some are HB donors, whereas others are HB acceptors for water.

Amino acid hydration is relevant for understanding the general properties of protein hydration in a host of arenas. Examples include enzymatic activity (117, 118), protein folding and association (88), protein stability (119, 120), and response to thermodynamic stress (121, 122). Not only are amino acids the building blocks of proteins, they are also intensively used either alone or assembled in short peptides for biomimicking, as for functionalized nanoparticles (123) or surfaces (124). Their aqueous solvation hence shapes the interfacial properties of such nanomaterials.

The importance of amino acid hydration has been understood early on (125, 126), and the different behavior of the hydrophilic and hydrophobic side chains was identified as the driving force in protein folding (127). The affinity of amino acids for water and other solvents has been measured experimentally (128, 129) and correlated with the partition of amino acids in folded protein structures (130, 131). Despite this significant progress, illustrated, e.g., by the establishment and now routine use of the hydrophobic scale of amino acid side chains (see, e.g., 132), the local water dynamics around them has not been extensively investigated, although important contributions have been made, some of which are now mentioned.

NMR experiments on simpler molecules possessing the typical hydrophilic chemical groups (amine, hydroxyl, carbonyl, and carboxylate groups) (75, 92, 133) indicate a moderate retardation for hydration shell water reorientation by a factor <3 compared to the bulk. A weak retardation (1.4–1.7) has been also measured for hydration water around amino acid–derived molecules with hydrophilic and amphiphilic character, respectively (22).

The local dynamics of reorientation around the side chains of isolated amino acids in water has been recently investigated in the framework of the EJM (134), with particular attention devoted to the different effects of the amino acid HB donor and acceptor sites. The MD simulation results yield direct estimates of the water jump times and have been interpreted microscopically via a TS free energy decomposition, as now discussed.

For amino acid HB donor groups, the reorientation dynamics of a neighboring water OH bond stems solely from an excluded-volume effect, as already observed for hydrophobic solutes

(see Section 3.2). The water HB exchange dynamics is only slightly retarded with respect to bulk water, with a retardation factor of $\sim$1.1–1.2.

For amino acid HB acceptor groups, the excluded-volume term is in fact not sufficient to properly describe the HB exchange kinetics. It is also necessary to include the asymmetry between the respective strengths of the initial HB with the amino acid group and of the final HB with a water oxygen. This HB asymmetry contribution, termed the transition-state hydrogen-bond (TSHB) factor, can be analytically described in the EJM. The HB strength is quantified via the potential of mean force between the reorienting water molecule and the acceptor site; the activation free energies to reach the jump TS geometry, i.e., to stretch the initial HB to its length in the TS, are computed both when starting from an HB donated to the amino acid site ($\Delta G_{aa}^{\ddagger}$) and in the bulk ($\Delta G_{bulk}^{\ddagger}$). Within a TS theory description, their difference $\Delta\Delta G^{\ddagger} = \Delta G_{aa}^{\ddagger} - \Delta G_{bulk}^{\ddagger}$ provides the accelerating/retarding factor for the HB exchange reaction due to the TSHB factor

$$\rho_{HB} = e^{\beta \Delta\Delta G^{\ddagger}}. \tag{5}$$

Combining this with the TSEV retardation factor due to the solute steric hindrance (80) gives a predictive model for the water jump HB exchange rate constant in a general case,

$$\tau_{jump} = \rho_V \cdot \rho_{HB} \cdot \tau_{jump}^{bulk}, \tag{6}$$

where τ_{jump} and τ_{jump}^{bulk} are the characteristic times for the HB exchange for water around the amino acid and in the bulk, respectively.

For the HB acceptor sites, three different situations occurred in the simulations (134). For the few cases involving a hydroxyl acceptor (serine, threonine, tyrosine), water reorientation is even faster than in the bulk. For carbonyl groups (asparagine, glutamine), reorientation is only slightly perturbed by the presence of the amino acid HB acceptor. Finally, for strong HB acceptors (histidine's nitrogen, and carboxylate oxygen molecules of aspartic and glutamic acids), the strongest retardation is observed (a factor between 2 and 4). With a proper estimate of the initial HB strength, the EJM describes all these cases well (**Figure 4c**). The comparison of the relative importance of the TSEV and TSHB factors for acceptor groups (**Figure 4d**) demonstrates the major role that can be played by the TSHB factor.

Amino acids also affect the diffusive frame reorientation contribution to water reorientation (see Equation 3). Whereas in bulk water and next to amino acid HB donor groups the relative frame contribution is $\sim$39%, it becomes slightly smaller for weak HB acceptor groups ($\sim$23%) and much greater for the glutamic and aspartic acid carboxylate groups ($\sim$54%). This increasing importance results from the increasing HB strength, which retards the HB jump exchange time and enhances the relative contribution of the frame tumbling reorientation.

3.3.3. Toward complex biosystems.
The study of water reorientation at the interface of complex molecular systems such as proteins and DNA is a natural further application of the EJM and of its analytical formulation, including the TSEV and TSHB effects for aqueous solutes. In proteins, additional challenges may arise: Water dynamics is affected by the surface local topology, i.e., its curvature (135), the presence of clefts and cavities (76, 136), and the differing free energetic interactions with the various exposed amino acid chemical groups.

The microscopic local description and quantification of water HB exchange based on an EJM approach should shed light on the hydration dynamics of biomolecules in which both energetic and steric disorder are present, causing the heterogeneous dynamics observed experimentally (27, 137, 138) and in computer simulations (81, 139–141). Moreover, the analytical formulation of the EJM and its components paves the way to an ab initio mapping of protein surfaces without the need to perform expensive simulations and analysis. Such a map would be key for accounting
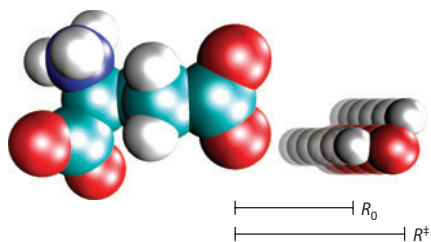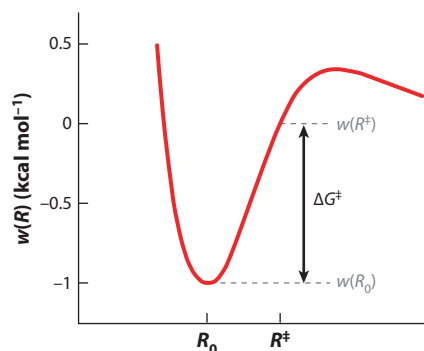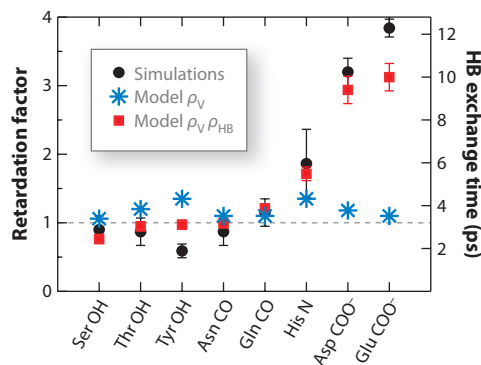
TSHB:
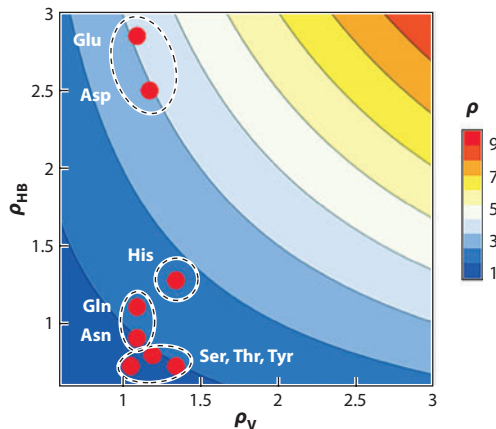transition-state hydrogen bond

Figure 4

Transition-state hydrogen-bond (TSHB) model. (*a*) Pictorial representation of the HB formed between a water molecule and the carboxylate group of glutamic acid. The equilibrium distance between the hydrogen-bonded oxygen molecules is R_0. The HB elongates by thermal fluctuation up to the value $R^{\ddagger}$ characterizing the TS. (*b*) The activation free energy to stretch the initial HB ($\Delta G^{\ddagger}$), evaluated through the potential of mean force for the bonded oxygen molecules. (*c*) Retardation factor with respect to the bulk of the HB exchange dynamics for amino acid HB acceptor sites, with results from simulations (*black circles*), from the TSEV model (*blue stars*), and from the combined transition-state excluded-volume (TSEV) and TSHB models (see Equation 6) (*red squares*) (134). (*d*). Contour plot of the overall retardation factor $\rho_V \cdot \rho_{HB}$ as a function of its TSEV and TSHB components with the values of amino acid HB acceptors.

for aqueous solvent effects in the prediction of protein/protein interfaces by individuating labile regions of the hydration layer (142). The hydration map should clearly reflect the distribution of different acceptor/donor sites and would be a useful tool for understanding, e.g., the protective role of the hydration skin around proteins, illustrated by the well-known enrichment in charged amino acids at thermostable protein surfaces (143), and the solubility of proteins, which can be enhanced via supercharging (144).

Biomolecular surfaces also act as confining media by altering the kinetics of water reorientation via the reduction of the accessibility to new water partners (80, 101) or by forcing jump events toward biomolecular sites rather than toward the bulk, thereby reducing hydration layer–bulk

exchanges. These phenomena could be crucial for understanding hydration dynamics in protein active sites or in DNA grooves, and the consequent modulation of ligand (drug) binding (117, 145).

4. CONCLUDING REMARKS

Above we review water reorientation in a wide range of contexts, focusing on a new image of a jump mechanism for the dynamics. Numerous examples of open questions and directions for future research are given, but many more could be added. The local environment for a water molecule near the air-water interface certainly differs from that in the bulk; does this significantly impact the reorientation mechanism and rate? Related questions can be raised for heterogeneous reactions at aqueous surfaces where water reorientation is important (146, 147). In the area of vibrational energy transfer, significant rotational excitation of a water molecule has recently been implicated in excited water bend vibration relaxation (itself a major component of the OH vibrational relaxation pathway) (148–150); does this superthermal energy distribution alter the thermal regime scenario? This small sampling of issues and those within suggest that unraveling the microscopic details of water reorientation will challenge physical chemists for some time to come.

SUMMARY POINTS

1. Water reorients in the bulk mainly through large-amplitude angular jumps and not diffusively.

2. Angular jumps occur through a concerted HB acceptor exchange mechanism.

3. Hydrophobic solutes induce a moderate ($\simeq \times 1.5$) retardation of water dynamics in dilute solutions and a more pronounced slowdown at high concentration, which can be both ascribed to a jump TSEV effect.

4. Hydrophilic groups accepting strong HBs from water induce a marked slowdown of the water dynamics, due to a TSHB strength effect.

5. Water OH stretch frequency dephasing originates mainly from transient HB breaking, i.e., failed jump attempts, whereas successful jumps bring a minor contribution.

6. The (second-order) orientation TCF and the anisotropy measured by ultrafast IR spectroscopy decay with the same rate, except in some situations (e.g., salt solutions) due to vibrational lifetime distribution effects.

DISCLOSURE STATEMENT

ACKNOWLEDGMENTS

LITERATURE CITED

1. Debye P. 1929. *Polar Molecules*. New York: Chem. Cat.

2. Gertner BJ, Whitnell RM, Wilson KR, Hynes JT. 1991. Activation to the transition-state: reactant and solvent energy flow for a model S_N2 reaction in water. *J. Am. Chem. Soc.* 113:74–87

3. Ando K, Hynes JT. 1995. HCl acid ionization in water: a theoretical modeling. *J. Mol. Liq.* 64:25–37

4. Ando K, Hynes JT. 1997. Molecular mechanism of HCl acid ionization in water: ab initio potential energy surfaces and Monte Carlo simulations. *J. Phys. Chem. B* 101:10464–78

5. Marx D, Tuckerman ME, Hutter J, Parrinello M. 1999. The nature of the hydrated excess proton in water. *Nature* 397:601–4

6. Berkelbach TC, Lee HS, Tuckerman ME. 2009. Concerted hydrogen-bond dynamics in the transport mechanism of the hydrated proton: a first-principles molecular dynamics study. *Phys. Rev. Lett.* 103:238302

7. Marx D, Chandra A, Tuckerman ME. 2010. Aqueous basic solutions: hydroxide solvation, structural diffusion, and comparison to the hydrated proton. *Chem. Rev.* 110:2174–216

8. Woutersen S, Emmerichs U, Bakker HJ. 1997. Femtosecond mid-IR pump-probe spectroscopy of liquid water: evidence for a two-component structure. *Science* 278:658–60

9. Nienhuys HK, van Santen RA, Bakker HJ. 2000. Orientational relaxation of liquid water molecules as an activated process. *J. Chem. Phys.* 112:8487–94

10. Gallot G, Bratos S, Pommeret S, Lascoux N, Leicknam JC, et al. 2002. Coupling between molecular rotations and OH···O motions in liquid water: theory and experiment. *J. Chem. Phys.* 117:11301–9

11. Steinel T, Asbury JB, Zheng JR, Fayer MD. 2004. Watching hydrogen bonds break: a transient absorption study of water. *J. Phys. Chem. A* 108:10957–94

12. Fecko CJ, Loparo JJ, Roberts ST, Tokmakoff A. 2005. Local hydrogen bonding dynamics and collective reorganization in water: ultrafast infrared spectroscopy of HOD/D_2O. *J. Chem. Phys.* 122:054506

13. Moilanen DE, Fenn EE, Lin YS, Skinner JL, Bagchi B, Fayer MD. 2008. Water inertial reorientation: hydrogen bond strength and the angular potential. *Proc. Natl. Acad. Sci. USA* 105:5295–300

14. Bakker HJ, Rezus YLA, Timmer RLA. 2008. Molecular reorientation of liquid water studied with femtosecond midinfrared spectroscopy. *J. Phys. Chem. A* 112:11523–34

15. Bakker HJ, Skinner JL. 2010. Vibrational spectroscopy as a probe of structure and dynamics in liquid water. *Chem. Rev.* 110:1498–517

16. Lipari G, Szabo A. 1980. Effect of librational motion on fluorescence depolarization and nuclear magnetic resonance relaxation in macromolecules and membranes. *Biophys. J.* 30:489–506

17. Lin YS, Pieniazek PA, Yang M, Skinner JL. 2010. On the calculation of rotational anisotropy decay, as measured by ultrafast polarization-resolved vibrational pump-probe experiments. *J. Chem. Phys.* 132:174505

18. Laage D, Hynes JT. 2007. Reorientational dynamics of water molecules in anionic hydration shells. *Proc. Natl. Acad. Sci. USA* 104:11167–72

19. Abragam A. 1961. *The Principles of Nuclear Magnetism*. Oxford, UK: Clarendon

20. Jonas J, Defried T, Wilbur DJ. 1976. Molecular motions in compressed liquid water. *J. Chem. Phys.* 65:582–88

21. Lang E, Lüdemann HD. 1977. Pressure and temperature-dependence of longitudinal proton relaxation times in supercooled water to −87°C and 2500 bar. *J. Chem. Phys.* 67:718–23

22. Qvist J, Halle B. 2008. Thermal signature of hydrophobic hydration dynamics. *J. Am. Chem. Soc.* 130:10345–53

23. Ropp J, Lawrence C, Farrar TC, Skinner JL. 2001. Rotational motion in liquid water is anisotropic: a nuclear magnetic resonance and molecular dynamics simulation study. *J. Am. Chem. Soc.* 123:8047–52

24. van der Maarel JRC, Lankhorst D, de Bleijser J, Leyte JC. 1986. Water dynamics in aqueous electrolyte solutions from proton, deuterium, and oxygen-17 nuclear magnetic relaxation. *J. Phys. Chem.* 90:1470–78

25. Bagno A, Rastrelli F, Saielli G. 2005. NMR techniques for the investigation of solvation phenomena and non-covalent interactions. *Prog. Nucl. Magn. Reson. Spectrosc.* 47:41–93

26. Teixeira J, Bellissent-Funel MC, Chen SH, Dianoux AJ. 1985. Experimental determination of the nature of diffusive motions of water molecules at low temperatures. *Phys. Rev. A* 31:1913–17

15. Recent overview of ultrafast infrared spectroscopy studies of water structure and dynamics.

22. NMR study of water dynamics around hydrophobes, and comparison with ultrafast infrared and QENS interpretations.

27. Russo D, Murarka RK, Copley JRD, Head-Gordon T. 2005. Molecular view of water dynamics near model peptides. *J. Phys. Chem. B* 109:12966–75

28. Di Cola D, Deriu A, Sampoli M, Torcini A. 1996. Proton dynamics in supercooled water by molecular dynamics simulations and quasielastic neutron scattering. *J. Chem. Phys.* 104:4223–32

29. Faraone A, Liu L, Chen SH. 2003. Model for the translation-rotation coupling of molecular motion in water. *J. Chem. Phys.* 119:6302–13

30. Laage D. 2009. Reinterpretation of the liquid water quasi-elastic neutron scattering spectra based on a nondiffusive jump reorientation mechanism. *J. Phys. Chem. B* 113:2684–87

31. Rønne C, Östrand PO, Keiding SR. 1999. THz spectroscopy of liquid H_2O and D_2O. *Phys. Rev. Lett.* 82:2888–91

32. Barthel J, Bachhuber K, Buchner R, Hetzenauer H. 1990. Dielectric spectra of some common solvents in the microwave region: water and lower alcohols. *Chem. Phys. Lett.* 165:369–73

33. Winkler K, Lindner J, Börsing H, Vöhringer P. 2000. Ultrafast Raman-induced Kerr effect of water: single molecule versus collective motions. *J. Chem. Phys.* 113:4674–82

34. Rønne C, Thrane L, Östrand PO, Wallqvist A, Mikkelsen KV, Keiding SR. 1997. Investigation of the temperature dependence of dielectric relaxation in liquid water by THz reflection spectroscopy and molecular dynamics simulation. *J. Chem. Phys.* 107:5319–31

35. Laage D, Hynes JT. 2008. On the molecular mechanism of water reorientation. *J. Phys. Chem. B* 112:14230–42

36. Pal S, Zewail A. 2004. Dynamics of water in biological recognition. *Chem. Rev.* 104:2099–123

37. Asbury JB, Steinel T, Kwak K, Corcelli SA, Lawrence CP, et al. 2004. Dynamics of water probed with vibrational echo correlation spectroscopy. *J. Chem. Phys.* 121:12431–46

38. Eaves JD, Loparo JJ, Fecko CJ, Roberts ST, Tokmakoff A, Geissler PL. 2005. Hydrogen bonds in liquid water are broken only fleetingly. *Proc. Natl. Acad. Sci. USA* 102:13019–22

39. Born B, Kim SJ, Ebbinghaus S, Gruedele M, Havenith M. 2009. The terahertz dance of water with the proteins: the effect of protein flexibility on the dynamical hydration shell of ubiquitin. *Faraday Discuss.* 141:161–73

40. Lawrence CP, Skinner JL. 2003. Vibrational spectroscopy of HOD in liquid D_2O. III. Spectral diffusion, and hydrogen-bonding and rotational dynamics. *J. Chem. Phys.* 118:264–72

41. Laage D, Hynes JT. 2006. A molecular jump mechanism of water reorientation. *Science* 311:832–35

42. Paesani F, Voth GA. 2009. The properties of water: insights from quantum simulations. *J. Phys. Chem. B* 113:5702–19

43. Sprik M, Hutter J, Parrinello M. 1996. Ab initio molecular dynamics simulation of liquid water: comparison of three gradient-corrected density functionals. *J. Chem. Phys.* 105:1142–52

44. Silvestrelli PL. 2009. Are there immobilized water molecules around hydrophobic groups? Aqueous solvation of methanol from first principles. *J. Phys. Chem. B* 113:10728–31

45. Rezus YLA, Bakker HJ. 2005. On the orientational relaxation of HDO in liquid water. *J. Chem. Phys.* 123:114502

46. Tan HS, Piletic IR, Fayer MD. 2005. Orientational dynamics of water confined on a nanometer length scale in reverse micelles. *J. Chem. Phys.* 122:174501

47. Laage D, Hynes JT. 2006. Do more strongly hydrogen-bonded waters reorient more slowly? *Chem. Phys. Lett.* 433:80–85

48. Piatkowski L, Eisenthal KB, Bakker HJ. 2009. Ultrafast intermolecular energy transfer in heavy water. *Phys. Chem. Chem. Phys.* 11:9033–38

49. Torii H. 2006. Time-domain calculations of the polarized raman spectra, the transient infrared absorption anisotropy, and the extent of delocalization of the OH stretching mode of liquid water. *J. Phys. Chem. A* 110:9469–77

50. Eisenberg D, Kauzmann W. 1969. *The Structure and Properties of Water*. London: Clarendon

51. Rossky PJ, Karplus M. 1979. Solvation: a molecular dynamics study of a dipeptide in water. *J. Am. Chem. Soc.* 101:1913–37

52. Rahman A, Stillinger FH. 1971. Molecular dynamics study of liquid water. *J. Chem. Phys.* 55:3336–59

38. 2D-IR study revealing the transient character of non-HB states in bulk water.

41. First detailed molecular description of the water reorientation mechanism through large angular jumps.

53. van der Spoel D, van Maaren PJ, Berendsen HJC. 1998. A systematic study of water models for molecular simulation: derivation of water models optimized for use with a reaction field. *J. Chem. Phys.* 108:10220–30

54. Bagchi B. 2005. Water dynamics in the hydration layer around proteins and micelles. *Chem. Rev.* 105:3197–219

55. Luzar A. 1996. Water hydrogen-bond dynamics close to hydrophobic and hydrophilic groups. *Faraday Discuss.* 103:29–40

56. Luzar A, Chandler D. 1996. Hydrogen-bond kinetics in liquid water. *Nature* 379:55–57

57. Sciortino F, Geiger A, Stanley HE. 1991. Effect of defects on molecular mobility in liquid water. *Nature* 354:218–21

58. Ivanov EN. 1964. Theory of rotational Brownian motion. *Soviet Phys. JETP* 18:1041–55

59. Berne BJ, Pecora R. 2000. *Dynamic Light Scattering with Applications to Chemistry, Biology, and Physics*. New York: Dover

60. Ohmine I, Tanaka H. 1993. Fluctuation, relaxations, and hydration in liquid water: hydrogen-bond rearrangement dynamics. *Chem. Rev.* 93:2545–66

61. Rapaport DC. 1983. Hydrogen bonds in water network organization and lifetimes. *Mol. Phys.* 50:1151–62

62. Luzar A. 2000. Resolving the hydrogen bond dynamics conundrum. *J. Chem. Phys.* 113:10663–75

63. Chandra A. 2000. Effects of ion atmosphere on hydrogen-bond dynamics in aqueous electrolyte solutions. *Phys. Rev. Lett.* 85:768–71

64. Stirnemann G, Laage D. 2010. Direct evidence of angular jumps during water reorientation through two-dimensional infrared anisotropy. *J. Phys. Chem. Lett.* 1:1511–15

65. **Moilanen DE, Wong D, Rosenfeld DE, Fenn EE, Fayer MD. 2009. Ion-water hydrogen-bond switching observed with 2D IR vibrational echo chemical exchange spectroscopy. *Proc. Natl. Acad. Sci. USA* 106:375–80**

66. Park S, Odelius M, Gaffney KJ. 2009. Ultrafast dynamics of hydrogen bond exchange in aqueous ionic solutions. *J. Phys. Chem. B* 113:7825–35

67. **Ji M, Odelius M, Gaffney KJ. 2010. Large angular jump mechanism observed for hydrogen bond exchange in aqueous perchlorate solution. *Science* 328:1003–5**

68. Rey R, Møller KB, Hynes JT. 2002. Hydrogen bond dynamics in water and ultrafast infrared spectroscopy. *J. Phys. Chem. A* 106:11993–96

69. Møller K, Rey R, Hynes J. 2004. Hydrogen bond dynamics in water and ultrafast spectroscopy: a theoretical study. *J. Phys. Chem. A* 108:1275–89

70. Nibbering ETJ, Elsaesser T. 2004. Ultrafast vibrational dynamics of hydrogen bonds in the condensed phase. *Chem. Rev.* 104:1887–914

71. Skinner JL, Auer BM, Lin YS. 2009. Vibrational line shapes, spectral diffusion, and hydrogen bonding in liquid water. *Adv. Chem. Phys.* 142:59–103

72. Stirnemann G, Hynes JT, Laage D. 2010. Water hydrogen bond dynamics in aqueous solutions of amphiphiles. *J. Phys. Chem. B* 114:3052–59

73. Fecko CJ, Eaves JD, Loparo JJ, Tokmakoff A, Geissler PL. 2003. Ultrafast hydrogen-bond dynamics in the infrared spectroscopy of water. *Science* 301:1698–702

74. **Endom L, Hertz HG, Thul B, Zeidler MD. 1967. A microdynamic model of electrolyte solutions as derived from nuclear magnetic relaxation and self-diffusion data. *Ber. Buns. Gesell.* 71:1008–31**

75. Hertz HG, Zeidler MD. 1964. Kernmagnetische Relaxationszeitmessungen zur Frage der Hydratation unpolarer Gruppen in wassriger Losung. *Ber. Buns. Gesell.* 68:821–35

76. Halle B. 2004. Protein hydration dynamics in solution: a critical survey. *Philos. Trans. R. Soc. Lond. B* 359:1207–24

77. Van-Quynh A, Willson S, Bryant RG. 2003. Protein reorientation and bound water molecules measured by ^{1}H magnetic spin-lattice relaxation. *Biophys. J.* 84:558–63

78. Kropman MF, Bakker HJ. 2001. Dynamics of water molecules in aqueous solvation shells. *Science* 291:2118–20

79. **Rezus YLA, Bakker HJ. 2007. Observation of immobilized water molecules around hydrophobic groups. *Phys. Rev. Lett.* 99:148301**

65. First measurement of the HB exchange time in an ionic aqueous solution via 2D-IR spectroscopy.

67. First measurement of the reorientation amplitude due to HB exchange in an ionic aqueous solution via 2D-IR spectroscopy.

74. Along with Ref. 75, pioneering NMR study of water dynamics around a broad range of solutes.

79. First time-resolved observation of water dynamics around hydrophobic solutes, concluding that some water molecules are immobilized.

80. **Laage D, Stirnemann G, Hynes JT. 2009. Why water reorientation slows without iceberg formation around hydrophobic solutes.** *J. Phys. Chem. B* **113:2428–35**

81. Abseher R, Schreiber H, Steinhauser O. 1996. The influence of a protein on water dynamics in its vicinity investigated by molecular dynamics simulation. *Proteins* 25:366–78

82. Laage D, Hynes JT. 2008. On the residence time for water in a solute hydration shell: application to aqueous halide solutions. *J. Phys. Chem. B* 112:7697–701

83. Ball P. 2008. Water as an active constituent in cell biology. *Chem. Rev.* 108:74–108

84. Blokzijl W, Engberts JBFN. 1993. Hydrophobic effects: opinions and facts. *Angew. Chem. Intl. Ed. Engl.* 32:1545–79

85. Chandler D. 2005. Interfaces and the driving force of hydrophobic assembly. *Nature* 437:640–47

86. Pratt L. 2002. Molecular theory of hydrophobic effects: "She is too mean to have her name repeated." *Annu. Rev. Phys. Chem.* 53:409–36

87. Berne BJ, Weeks JD, Zhou R. 2009. Dewetting and hydrophobic interaction in physical and biological systems. *Annu. Rev. Phys. Chem.* 60:85–103

88. Levy Y, Onuchic J. 2006. Water mediation in protein folding and molecular recognition. *Annu. Rev. Biophys. Biomol. Struct.* 35:389–415

89. Ashbaugh HS, Truskett TM, Debenedetti PG. 2002. A simple molecular thermodynamic theory of hydrophobic hydration. *J. Chem. Phys.* 116:2907–21

90. Graziano G. 2006. Scaled particle theory study of the length scale dependence of cavity thermodynamics in different liquids. *J. Phys. Chem. B* 110:11421–26

91. Haselmeier R, Holz M, Marbach W, Weingartner H. 1995. Water dynamics near a dissolved noble gas: first direct experimental evidence for a retardation effect. *J. Phys. Chem.* 99:2243–46

92. Ishihara Y, Okouchi S, Uedaira H. 1997. Dynamics of hydration of alcohols and diols in aqueous solutions. *J. Chem. Soc. Faraday Trans.* 93:3337–42

93. Shimizu A, Fumino K, Yukiyasu K, Taniguchi Y. 2000. NMR studies on dynamic behavior of water molecule in aqueous denaturant solutions at 25°C: effects of guanidine hydrochloride, urea and alkylated ureas. *J. Mol. Liq.* 85:269–78

94. Yoshida K, Ibuki K, Ueno M. 1998. Pressure and temperature effects on H-2 spin-lattice relaxation times and H-1 chemical shifts in tert-butyl alcohol- and urea-D_2O solutions. *J. Chem. Phys.* 108:1360–67

95. Frank HS, Evans MW. 1945. Free volume and entropy in condensed systems: III. Entropy in binary liquid mixtures—partial molar entropy in dilute solutions—structure and thermodynamics of electrolytes. *J. Chem. Phys.* 13:507–32

96. Buchanan P, Aldiwan N, Soper A, Creek J, Koh C. 2005. Decreased structure on dissolving methane in water. *Chem. Phys. Lett.* 415:89–93

97. Hummer G, Garde S, Garca AE, Pohorille A, Pratt LR. 1996. An information theory model of hydrophobic interactions. *Proc. Natl. Acad. Sci. USA* 93:8951–55

98. Bakulin AA, Liang C, Jansen TLC, Wiersma DA, Bakker HJ, Pshenichnikov MS. 2009. Hydrophobic solvation: a 2D IR spectroscopic inquest. *Acc. Chem. Res.* 42:1229–38

99. Bonn M, Bakker HJ, Rago G, Pouzy F, Siekierzycka JR, et al. 2009. Suppression of proton mobility by hydrophobic hydration. *J. Am. Chem. Soc.* 131:17070–71

100. Hallenga K, Grigera J, Berendsen H. 1980. Influence of hydrophobic solutes on the dynamic behavior of water. *J. Phys. Chem.* 84:2381–90

101. Xu H, Berne B. 2001. Hydrogen-bond kinetics in the solvation shell of a polypeptide. *J. Phys. Chem. B* 105:11929–32

102. Stirnemann G, Rossky PJ, Hynes JT, Laage D. 2010. Water reorientation, hydrogen-bond dynamics and 2D-IR spectroscopy next to an extended hydrophobic surface. *Faraday Discuss.* 146:263–81

103. Almasy L, Len A, Szekely NK, Plestil J. 2007. Solute aggregation in dilute aqueous solutions of tetramethylurea. *Fluid Phase Equilib.* 257:114–19

104. Holz M, Grunder R, Sacco A, Meleleo A. 1993. Nuclear-magnetic-resonance study of self-association of small hydrophobic solutes in water: salt effects and the lyotropic series. *J. Chem. Soc. Faraday Trans.* 89:1215–22

105. Petersen C, Tielrooij KJ, Bakker HJ. 2009. Strong temperature dependence of water reorientation in hydrophobic hydration shells. *J. Chem. Phys.* 130:214511

106. Fumino K, Yukiyasu K, Shimizu A, Taniguchi Y. 1998. NMR studies on dynamic behavior of water molecules in tetraalkylammonium bromide-D_2O solutions at 5–25°C. *J. Mol. Liq.* 75:1–12

107. Nakahara M, Wakai C, Yoshimoto Y, Matubayasi N. 1996. Dynamics of hydrophobic hydration of benzene. *J. Phys. Chem.* 100:1345–49

108. Allesch M, Schwegler E, Galli G. 2007. Structure of hydrophobic hydration of benzene and hexafluorobenzene from first principles. *J. Phys. Chem. B* 111:1081–89

109. Ohtaki H, Radnai T. 1993. Structure and dynamics of hydrated ions. *Chem. Rev.* 93:1157–204

110. Gouaux E, MacKinnon R. 2005. Principles of selective ion transport in channels and pumps. *Science* 310:1461–65

111. Bakker HJ, Kropman MF, Omta AW. 2005. Effect of ions on the structure and dynamics of liquid water. *J. Phys. Condens. Matter* 17:S3215–24

112. Boisson J. 2008. *Sur l'interaction eau/anion; les caractères structurants et déstructurants, la rupture de symétrie du nitrate*. PhD thesis. ENS-Paris VI

113. Masia M, Rey R. 2005. Diffusion coefficient of ionic solvation shell molecules. *J. Chem. Phys.* 122:094502

114. Bakker HJ. 2008. Structural dynamics of aqueous salt solutions. *Chem. Rev.* 108:1456–73

115. Marcus Y. 2009. Effect of ions on the structure of water: structure making and breaking. *Chem. Rev.* 108:1346–70

116. Nigro B, Re S, Laage D, Rey R, Hynes JT. 2006. On the ultrafast infrared spectroscopy of anion hydration shell hydrogen bond dynamics. *J. Phys. Chem. A* 110:11237–43

117. Abel R, Young T, Farid R, Berne BJ, Friesner RA. 2008. Role of the active-site solvent in the thermodynamics of factor Xa ligand binding. *J. Am. Chem. Soc.* 130:2817–31

118. Knight JDR, Hamelberg D, McCammon JA, Kothary R. 2009. The role of conserved water molecules in the catalytic domain of protein kinases. *Proteins* 76:527–35

119. Dunitz JD. 1994. The entropic cost of bound water in crystals and biomolecules. *Science* 264:670

120. Angel TE, Chance MR, Palczewski K. 2009. Conserved waters mediate structural and functional activation of family A (rhodopsin-like) G protein-coupled receptors. *Proc. Natl. Acad. Sci. USA* 106:8555–60

121. Collins MD, Hummer G, Quillin ML, Matthews BW, Gruner SM. 2005. Cooperative water filling of a nonpolar protein cavity observed by high-pressure crystallography and simulation. *Proc. Natl. Acad. Sci. USA* 102:16668–71

122. Sterpone F, Bertonati C, Briganti G, Melchionna S. 2009. Key role of proximal water in regulating thermostable proteins. *J. Phys. Chem. B* 113:131–37

123. De M, You CC, Srivastava S, Rotello VM. 2007. Biomimetic interactions of proteins with functionalized nanoparticles: a thermodynamic study. *J. Am. Chem. Soc.* 129:10747–53

124. Sarikaya M, Tamerler C, Jen AKY, Schulten K, Baneyx F. 2003. Molecular biomimetics: nanotechnology through biology. *Nat. Mater.* 2:577–85

125. Kauzmann W. 1959. Some factors in the interpretation of protein denaturation. *Adv. Protein. Chem.* 14:1–63

126. Tanford C. 1962. Contribution of hydrophobic interactions to the stability of the globular conformation of proteins. *J. Am. Chem. Soc.* 84:4240–47

127. Tanford C. 1997. How protein chemists learned about the hydrophobic factor. *Protein Sci.* 6:1358–66

128. Nozaki Y, Tanford C. 1971. The solubility of amino acids and two glycine peptides in aqueous ethanol and dioxane solutions: establishment of a hydrophobicity scale. *J. Biol. Chem.* 246:2211–17

129. Wolfenden R, Andersson L, Cullis PM, Southgate CC. 1981. Affinities of amino acid side chains for solvent water. *Biochemistry* 20:849–55

130. Perutz MF. 1965. Structure and function of haemoglobin: I. A tentative atomic model of horse oxyhaemoglobin. *J. Mol. Biol.* 13:646–68

131. Chothia C. 1976. The nature of the accessible and buried surfaces in proteins. *J. Mol. Biol.* 105:1–12

132. Kyte J, Doolittle RF. 1982. A simple method for displaying the hydropathic character of a protein. *J. Mol. Biol.* 157:105–32

133. Okouchi S, Moto T, Ishihara Y, Numajiri H, Uedaira H. 1996. Hydration of amines, diamines, polyamines and amides studied by NMR. *J. Chem. Soc. Faraday Trans.* 92:1853–57

134. Extension of the EJM to hydrophilic solutes, showing the key role of the initial HB acceptor.

134. **Sterpone F, Stirnemann G, Hynes JT, Laage D. 2010. Water hydrogen-bond dynamics around amino acids: the key role of hydrophilic hydrogen-bond acceptor groups. *J. Phys. Chem. B* 114:2083–89**

135. Cheng YK, Rossky PJ. 1998. Surface topography dependence of biomolecular hydrophobic hydration. *Nature* 392:696–99

136. Makarov VA, Andrews BK, Smith PE, Pettitt BM. 2000. Residence times of water molecules in the hydration sites of myoglobin. *Biophys. J.* 79:2966–74

137. Zhang L, Wang L, Kao YT, Qiu W, Yang Y, et al. 2007. Mapping hydration dynamics around a protein surface. *Proc. Natl. Acad. Sci. USA* 104:18461–66

138. Mattea C, Qvist J, Halle B. 2008. Dynamics at the protein-water interface from ^{17}O spin relaxation in deeply supercooled solutions. *Biophys. J.* 95:2951–63

139. Schröder C, Rudas T, Boresch S, Steinhauser O. 2006. Simulation studies of the protein-water interface. I. Properties at the molecular resolution. *J. Chem. Phys.* 124:234907

140. Bizzarri AR, Cannistraro S. 2002. Molecular dynamics of water at the protein-solvent interface. *J. Phys. Chem. B* 106:6617–33

141. Pizzitutti F, Marchi M, Sterpone F, Rossky PJ. 2007. How protein surfaces induce anomalous dynamics of hydration water. *J. Phys. Chem. B* 111:7584–90

142. Zhou H, Qin S. 2007. Interaction-sites prediction for protein complexes: a critical assessment. *Bioinformatics* 23:2203–9

143. Vieille C, Zeikus GJ. 2001. Hyperthermophilic enzymes: sources, uses, and molecular mechanisms for thermostability. *Microbiol. Mol. Biol. Rev.* 65:1–43

144. Lawrence MS, Phillips KJ, Liu DR. 2007. Supercharging proteins can impart unusual resilience. *J. Am. Chem. Soc.* 129:10110–12

145. Mukherjee A, Lavery R, Bagchi B, Hynes JT. 2008. On the molecular mechanism of drug intercalation into DNA: a simulation study of the intercalation pathway, free energy, and DNA structural changes. *J. Am. Chem. Soc.* 130:9747–55

146. Wang S, Bianco R, Hynes JT. 2009. Depth-dependent dissociation of nitric acid at an aqueous surface: Car-Parrinello dynamics. *J. Phys. Chem. A* 122:1295–307

147. Koch D, Toubin C, Peslherbe G, Hynes JT. 2008. Theoretical study of the formation of the aminoacetonitrile precursor of glycine on icy grain mantles in the interstellar medium. *J. Phys. Chem. C* 112:12972–80

148. Ingrosso F, Rey R, Elsaesser T, Hynes JT. 2009. Ultrafast energy transfer from the intramolecular bending vibration to librations in liquid water. *J. Phys. Chem. A* 113:6657–65

149. Rey R, Ingrosso F, Elsaesser T, Hynes JT. 2009. Pathways for H_2O bend vibrational relaxation in liquid water. *J. Phys. Chem. A* 113:8949–62

150. Kandratsenka A, Schroeder J, Schwarzer D, Vikhrenko V. 2009. Nonequilibrium molecular dynamics simulations of vibrational energy relaxation of HOD in D_2O. *J. Chem. Phys.* 130:174507

**Annual Review of
Physical Chemistry**

Volume 62, 2011

Contents

Indexes

Errata

An online log of corrections to *Annual Review of Physical Chemistry* articles may be
found at http://physchem.annualreviews.org/errata.shtml